High Electrochemical Performance Based on TiO_2 Nanobelt@Few-Layer MoS_2 Structure for Lithium-Ion Batteries

Minglei Mao,[a,b] Lin Mei,[a] Di Guo,[a] Lichen Wu,[a] Dan Zhang,[c] Qiuhong Li*[b] and Taihong Wang*[a]

[a] *Key Laboratory for Micro-Nano Optoelectronic Devices of Ministry of Education, State Key Laboratory for Chemo/Biosensing and Chemometrics, Hunan University, Changsha 410082, P. R. China, E-mail: thwang@iphy.ac.cn*

[b] *Pen-Tung Sah Institute of Micro-Nano Science and Technology of Xiamen University, Xiamen, 361005, China. E-mail: liqiuhong2004@hotmail.com*

[c] *Department of Electronic Engineering, School of Information Science and Engineering, Xiamen University, Xiamen 361005, China*

Supporting Information

Experimental Section

Chemicals: Titania P25 (TiO_2; ca. 80% anatase and 20% rutile), sodium hydroxide (NaOH), hydrochloric acid (HCl), sulfuric acid (H_2SO_4), ethylene glycol ($HOCH_2CH_2OH$), sodium molybdate ($Na_2MoO_4 \cdot 2H_2O$) and thioacetamide (C_2H_5NS) were purchased from Sigma-Aldrich Co. LLC. All chemicals were used without further purification. Deionized water was used throughout this study.

Synthesis of TiO_2 Nanobelts: TiO_2 nanobelts with rough surface were synthesized through a simple hydrothermal procedure followed by acid corrosion treatment.[1, 2] In a typical reaction, 0.1 g of TiO_2 powder (P25) was mixed with 20 mL of 10 M NaOH aqueous solution. The mixed solution was stirred and then transferred into a Teflon-lined stainless steel autoclave, heated at 180 °C for 48 h, and then air-cooled to room temperature. The obtained $Na_2Ti_3O_7$ powder was washed thoroughly with deionized water followed by a filtration process. The obtained wet powder was immersed in 0.1 mol/L HCl aqueous solution for 24 h and then washed thoroughly with distilled water to obtain the H-titanate ($H_2Ti_3O_7$) nanobelts. To obtain the rough surface, the H-titanate nanobelts were added into a 25 mL Teflon vessel, then filled with 0.02 M H_2SO_4 aqueous solution up to 80% of the total volume and maintained at 100 °C for 12 h. Finally, the products were isolated from the solution by centrifugation and sequentially washed with deionized water for several times, and dried at 70 °C for 10 h. By annealing the acid-corroded H-titanate at 600 °C for 2 h, the anatase TiO_2 nanobelts with rough surface were obtained.

Synthesis of TiO_2@MoS_2 structure: The formation process of TiO_2@MoS_2 hierarchical structures was described as follows. Typically, 30 mg sodium molybdate ($Na_2MoO_4 \cdot 2H_2O$) and 60 mg thioacetamide (C_2H_5NS) were dissolved in 20 mL deionized water to form a transparent solution. Then 20 mg TiO_2 nanobelts powder was added into the above solution and stirred to form the suspension. The solution was transferred to a Teflon-lined stainless steel autoclave and then heated in an electric oven at 220 °C for 24 h. A black product, TiO_2@MoS_2

structure, was harvested after centrifugation and dried at 50 °C for 12 h. For comparison, pure MoS_2 nanosheets were synthesized under the same conditions without the presence of TiO_2 nanobelts (Figure S1d).

Characterization: Field emission scanning electron microscopy (FESEM, Model JSM-7600F, JEOL Ltd., Tokyo, Japan) was used to characterize the morphologies and size of the synthesized samples. The chemical composition was investigated by the energy dispersive spectroscopy (EDS). High resolution transmission electron microscopy (HRTEM) images were carried out with a JOEL JEM 2100F microscope. X-ray powder diffraction (XRD) patterns were recorded on a Bruke D8 Advance powder X-ray diffractometer with Cu Kα (λ =0.15406 nm). X-ray photoelectron spectroscopy (XPS) was performed using an ESCALAB 250.

To evaluate the electrochemical performance of the TiO_2@MoS_2 structure, coin-type cells were assembled in an Argon-filled glove box. For preparing the working electrodes, the active material, carbon black and carboxyl methyl cellulose (CMC) were mixed in a weight ratio of 80:10:10, and in distilled water and absolute alcohol mixture, stirred at a constant speed for 12 h in order to form a homogeneous slurry, which was spread uniformly on a copper foil. The coated copper foil was cut into round pieces with a diameter of 1 cm, dried at 80 ˚C in a vacuum overnight. A Celgard 2400 microporous polypropylene membrane was used as a separator. The electrolyte contained a solution of 1 M $LiPF_6$ in ethylene carbonate/dimethyl carbonate/diethyl carbonate (1:1:1, in wt%). These cells were assembled in the glovebox (Super 1220/750, Switzerland) filled with highly pure argon gas (O_2 and H_2O levels less than 1 ppm). The cells were aged for 12 h before the measurements to ensure percolation of the electrolyte to the electrodes. The cyclic voltammetry and galvanostatic cycling was performed using an Arbin BT2000 system in the voltage of 0.01-3.0 V (vs Li^+/Li). Nyquist plots were recorded using a Zahner IM6 electrochemical work station.

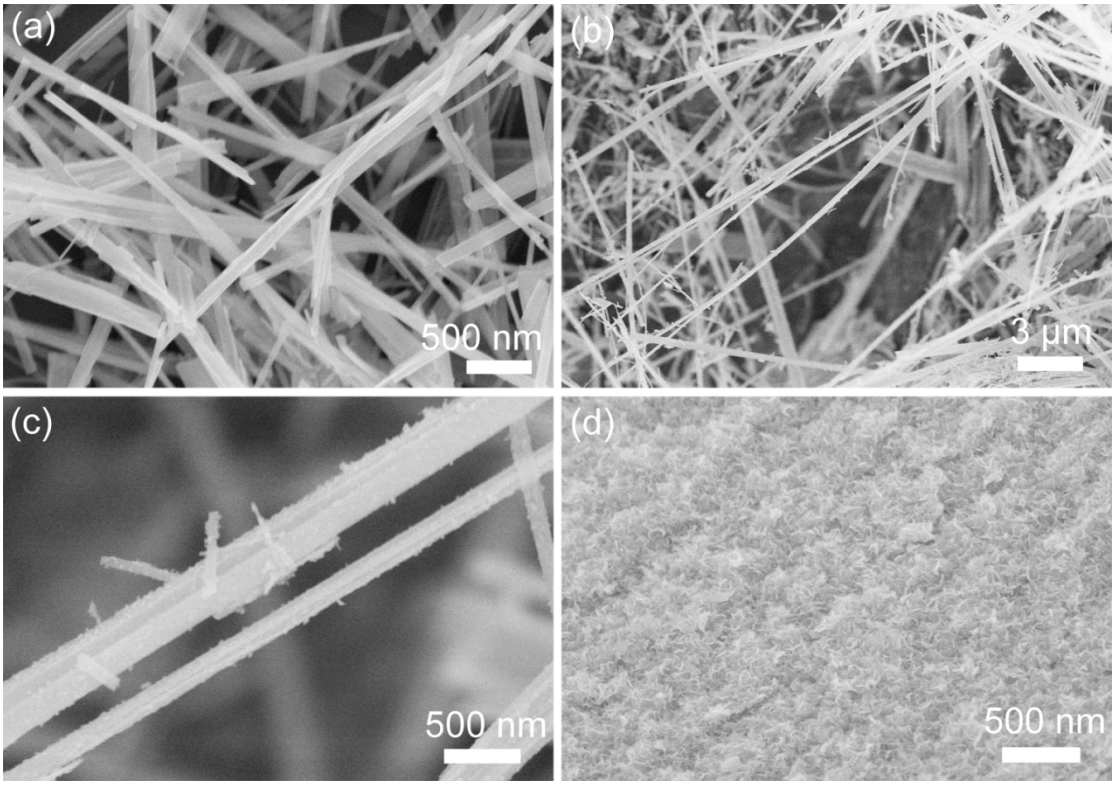

Figure S1. SEM images of TiO_2 nanobelts (a) before, (b) and (c) after acid treatment. (d) pure MoS_2 nanosheets.

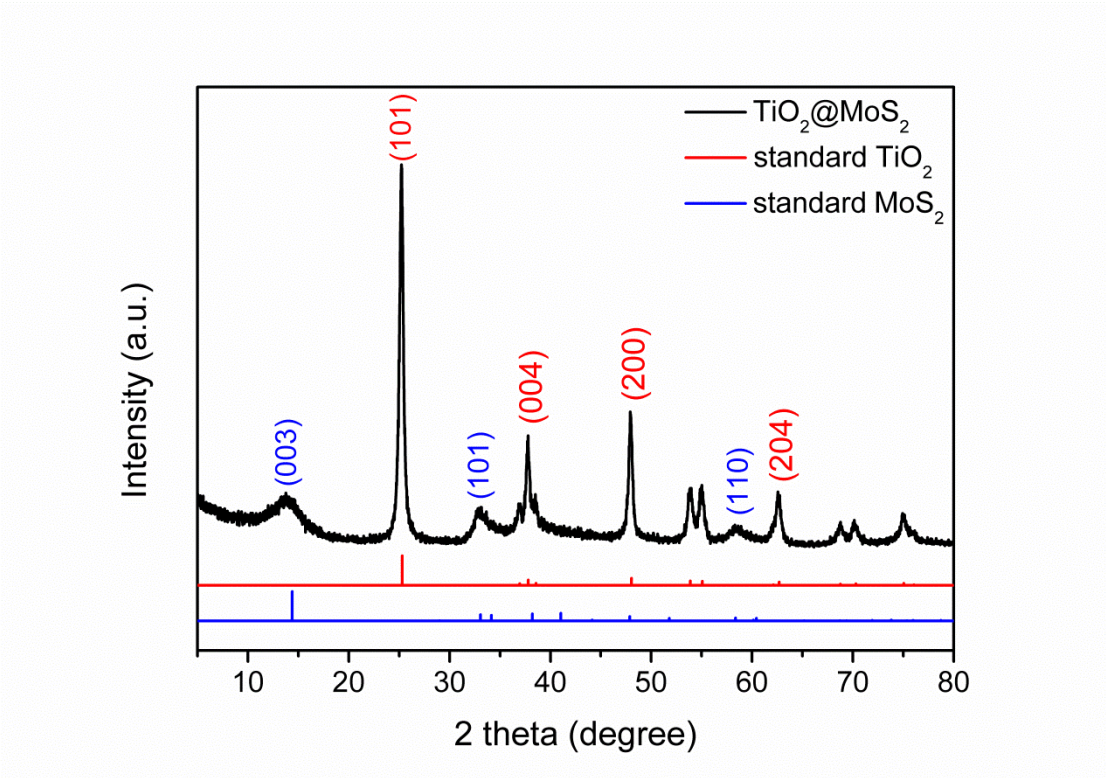

Figure S2. XRD patterns of TiO_2@MoS_2 structures.

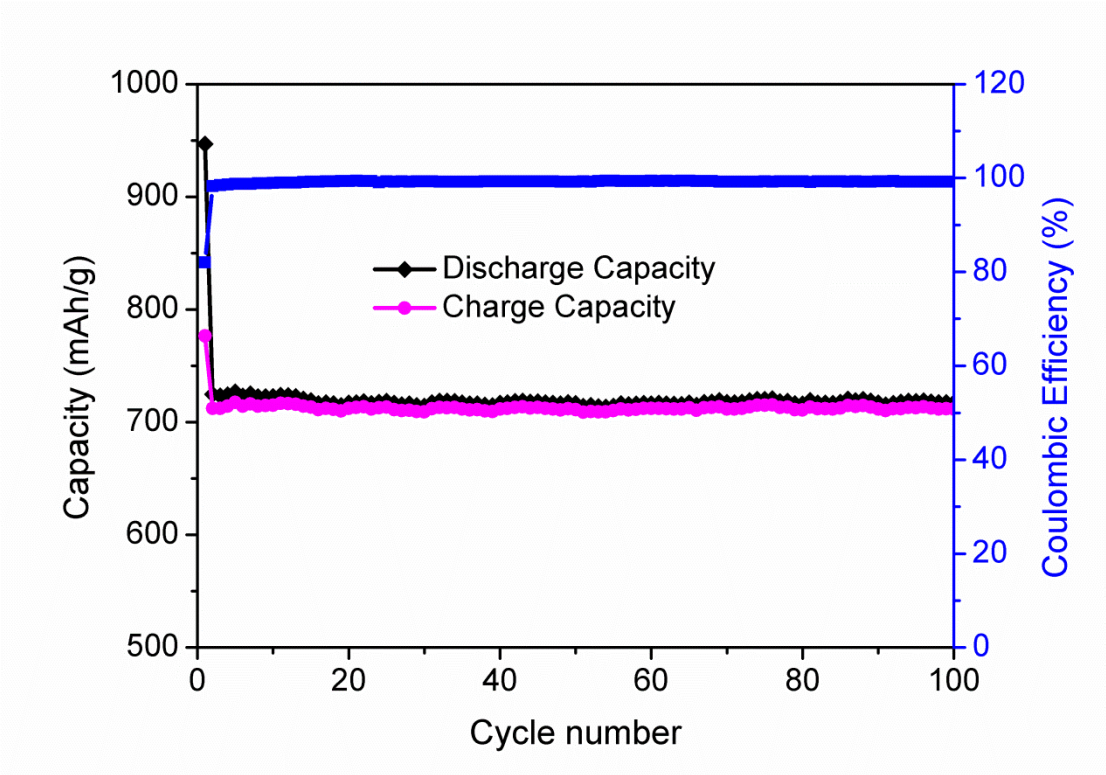

Figure S3. Cycling performance and Coulombic efficiency of TiO_2@MoS_2 tested at a current density of 100 mA/g in the range of 0.01-3V vs Li^+/Li.

Table 1 Recently reported Li-ion battery systems based on MoS_2 and TiO_2

Materials	Discharge Capacity (mAh/g)	Current Density (mA/g)	Ref.
MoS_2 flakes	300 (after 60 cycles)	100	3
	129	1000	
MoS_2 nanoflowers	531 (after 100 cycles)	100	4
	740	400	
MoS_2 microsphere	585 (after 70 cycles)	100	5
	353	1000	
MoS_2/Polyaniline	960 (charge) (after 50 cycles)	100	6
	320 (charge)	1000	
C-MoS_2	621 (after 80 cycles)	200	7
	550	1000	
CNT@ MoS_2	698 (after 60 cycles)	100	3
	369	1000	
TiO_2	174 (after 100 cycles)	1 C	8
	95	20 C	
TO/GS	199 (after 100 cycles)	1 C	9
	97	50 C	
$Li_4Ti_5O_{12}$-TiO_2-C	110 (after 100 cycles)	10 C	10
	166	0.5 C	
TiO_2@TiO_xN_y/TiN-GS	165 (after 100 cycles)	C/3	11
	130	12 C	
TiO_2@MoS_2	710 (charge) (after 100 cycles)	100	This work
	417 (charge)	1000	

Figure S4 shows the Nyquist plots of initial TiO_2@MoS_2 and that after 10 cycles. The diameter of the semi-circle at high frequencies is reduced in the plot of TiO_2@MoS_2 after 10 cycles, compared with that of initial TiO_2@MoS_2, indicating the decreased charge-transfer resistance at the electrode/electrolyte interface after 10 cycles. The enhanced conductivity facilitates the electron and Li^+ ion transfer in the electrode. Moreover, a slope line at the low frequency region represents the Warburg impendence (Z_w) caused by the lithium diffusion in electrodes. It is found that the transfer resistance of the initial TiO_2@MoS_2 is smaller than that after 10 cycles, which might be attributed to the increased interlayer distance of MoS_2.

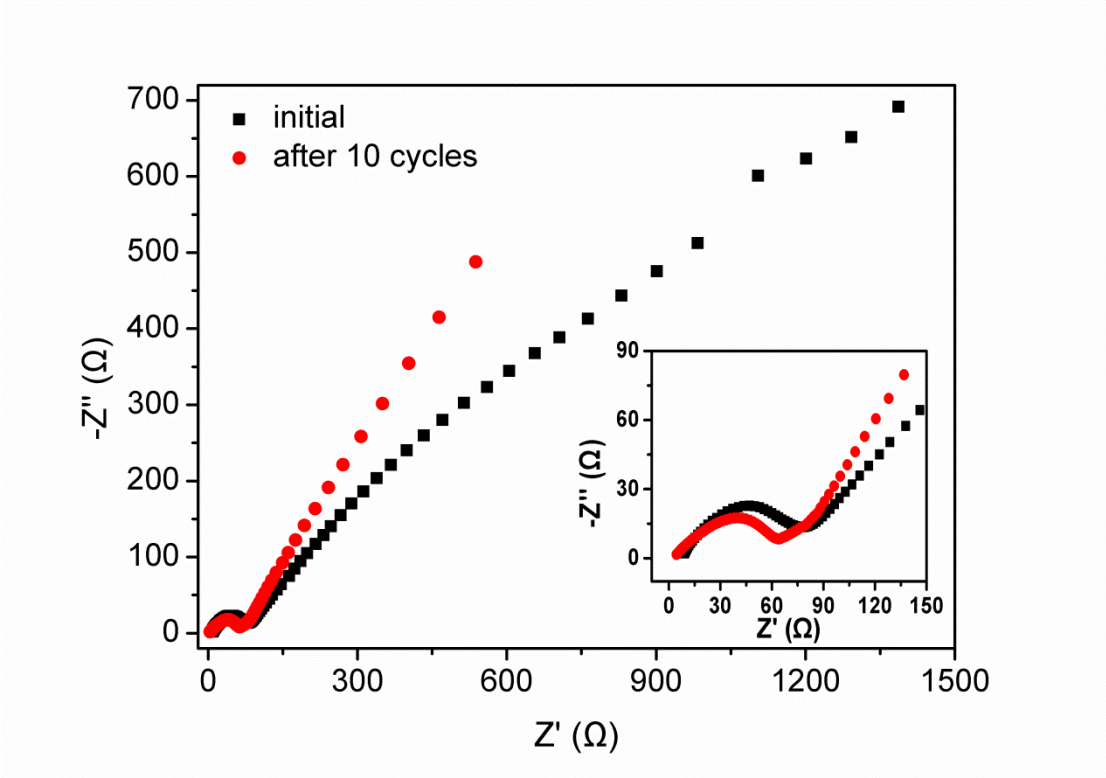

Figure S4. Nyquist plots (100 kHz-0.01Hz) of TiO_2@MoS_2 for the initial and 10th cycles.

Figure S5 represents the SEM and TEM images of TiO_2@MoS_2 after 100 cycles of charge-discharge. It is obvious that even after 100 cycles, TiO_2@MoS_2 almost retains its morphological characteristics, indicating that intercalation and conversion reactions of TiO_2@MoS_2 are quite reversible.

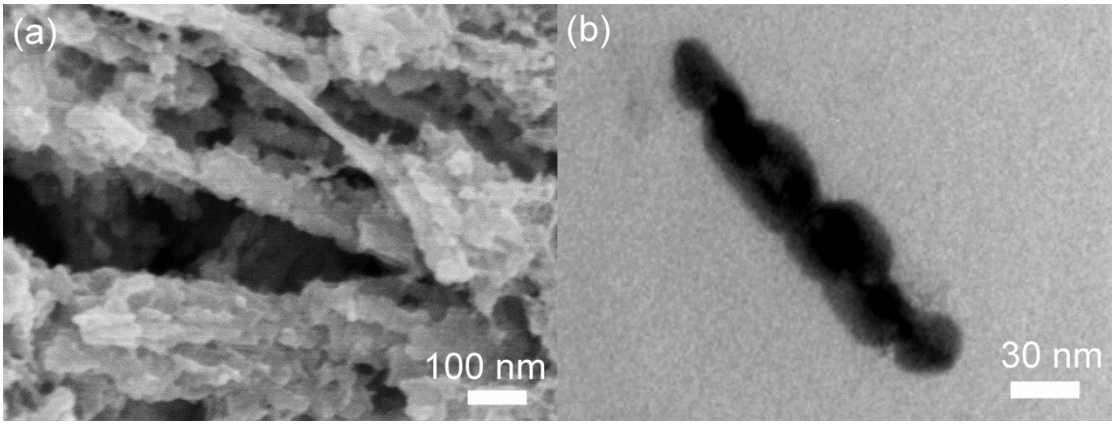

Figure S5. (a) SEM and (b) TEM images of TiO_2@MoS_2 after 100 cycles performance as anode in LIBs.

References

1. W. Zhou, G. Du, P. Hu, G. Li, D. Wang, H. Liu, J. Wang, R. I. Boughton, D. Liu and H. Jiang, *Journal of Materials Chemistry*, 2011, 21, 7937-7945.
2. Y. Wang, G. Du, H. Liu, D. Liu, S. Qin, N. Wang, C. Hu, X. Tao, J. Jiao, J. Wang and Z. L. Wang, *Advanced Functional Materials*, 2008, 18, 1131-1137.
3. S. Ding, J. S. Chen and X. W. Lou, *Chemistry – A European Journal*, 2011, 17, 13142-13145.
4. H. Li, W. Li, L. Ma, W. Chen and J. Wang, *Journal of Alloys and Compounds*, 2009, 471, 442-447.
5. S. Ding, D. Zhang, J. S. Chen and X. W. Lou, *Nanoscale*, 2012, 4, 95-98.
6. L. Yang, S. Wang, J. Mao, J. Deng, Q. Gao, Y. Tang and O. G. Schmidt, *Advanced Materials*, 2013, 25, 1180-1184.
7. C. Zhang, H. B. Wu, Z. Guo and X. W. Lou, *Electrochemistry Communications*, 2012, 20, 7-10.
8. J. S. Chen, Y. L. Tan, C. M. Li, Y. L. Cheah, D. Luan, S. Madhavi, F. Y. C. Boey, L. A. Archer and X. W. Lou, *Journal of the American Chemical Society*, 2010, 132, 6124-6130.
9. N. Li, G. Liu, C. Zhen, F. Li, L. Zhang and H.-M. Cheng, *Advanced Functional Materials*, 2011, 21, 1717-1722.
10. M. M. Rahman, J.-Z. Wang, M. F. Hassan, D. Wexler and H. K. Liu, *Advanced Energy Materials*, 2011, 1, 212-220.
11. Y. Qiu, K. Yan, S. Yang, L. Jin, H. Deng and W. Li, *ACS Nano*, 2010, 4, 6515-6526.